

# MODELING OF PROOF TEST LEVEL FLAWS USING CUBE CORNER INDENTS

S.L. Semjonov<sup>\*^</sup>, G.S. Glaesemann<sup>#</sup>, C.R. Kurkjian<sup>+</sup> and M.M. Bubnov<sup>\*</sup>

\* FORC, GPI, Russian Academy of Sciences, Moscow, Russia

# Corning, Inc, Corning, New York 14831

+ Bellcore, Morristown, New Jersey 07960

^ Work performed while on leave at Bellcore

## ABSTRACT

Proof test level flaws in lightguide fibers have been modeled using radial cracks in flat silica fibers. These cracks were produced using a diamond cube corner indenter with loads from 0.2 to 10 grams. Room temperature strengths ( $\sigma_{RT}$ ) from 150 to 500 MPa with Weibull  $m$ -values of 30-70 were obtained (stress rate ( $\dot{\sigma}$ ) = 0.12 GPa/s). It was found that  $\sigma_{RT} \sim P^{-1/3}$  as predicted theoretically. The ratio of liquid nitrogen to room temperature strengths ( $\sigma_{LN_2}/\sigma_{RT}$ ) was found to be approximately 2. The strengths of these indented fibers were measured at high stress rates. In these tests the strength appears to saturate at approximately the liquid nitrogen value at approximately  $10^4$  GPa/s). The full strength/stress rate curve can be approximated by a two-region semi-log plot. This indicates that the two region model suggested by Glaesemann et al<sup>1,2</sup>, is real.

## INTRODUCTION

Most standard telecommunication lightguide fibers now are proof tested at 700 MPa. This strength corresponds to a flaw size of  $\sim 1 \mu\text{m}$ . The high quality fibers produced today rarely have such flaws and thus it is difficult to study them in detail. However, since an understanding of these flaws is important for the prediction of the lifetime of such fibers, synthetically produced flaws usually are employed. Such flaws have been produced both by abrasion<sup>3,4</sup> and by the fusion of refractory particles<sup>5,6</sup> onto the fiber surface. Both techniques show a rather broad distribution of strengths and therefore they contain a broad distribution of flaw sizes. While it has been suggested that real production fibers may in fact contain a very wide distribution of flaw behavior<sup>7</sup>, it is necessary to study simple flaw types separately in order to understand their behavior fully. For these reasons, we have chosen to study a well-characterized proof test level flaw – one produced by indentation with a diamond

cube corner indenter. Using indenting loads from 0.2 to 10 grams we are able to span the range of strengths of interest.

The normal model for the study and prediction of fiber lifetimes is a single region power law model. Recently Glaesemann, et al.<sup>1,2</sup> have suggested the existence of a region II-like behavior in abraded ( $\sim 700$  MPa) fibers. This gives rise to two values of  $n$  (the stress corrosion susceptibility factor) and  $B$  (the strength retention factor). It is very important to verify this finding since it has substantial impact on the lifetime predictions of such fibers.

## EXPERIMENTAL

Fibers with two flat sides were drawn especially for these experiments in order to simplify the indentation process. The polymer coating was removed with hot sulfuric acid from 2-3 cm of the center of the fiber sample and a single indent was made. Indentations were made using a low load indentation instrument<sup>8</sup> and a diamond cube corner indenter<sup>9</sup>. This indenter produces a triangular-shaped impression with radial cracks extending from the three corners. The indentation was made so that one of the radial cracks was perpendicular to the fiber axis. A drop of ink on the fiber surface near the indent enabled one to locate the position of the indentation. Tensile strength measurements at moderate stress rates were made with a commercial tensile tester<sup>10</sup> and static fatigue measurements were made using a set-up as described by Krause<sup>11</sup>. The high stress rate measurements were made with the instrument described by Glaesemann<sup>2,12</sup>.

## RESULTS

Figure 1 shows a Weibull plot of room temperature strength ( $\dot{\sigma} \sim 0.12$  GPa/s) for various indentation loads. Figure 2 is a plot of strength versus indentation load. As indicated earlier<sup>13</sup>, loads which result in a given strength are two orders of magnitude less with a cube

corner indenter than with a Vickers indenter. It can be seen that the theoretically expected<sup>14</sup>  $\sigma \sim P^{-1/3}$  relation is obeyed. Figures 3 and 4 show AFM and SEM images of these indents. Figure 5 is a combined plot of dynamic and static fatigue at room temperature and approximately 50 % relative humidity. This is a power law (log-log) plot and indicates that within experimental error two n-values are required. While it might be expected that a semi-log (exponential) plot would give a single straight line, this was found not to be the case (see Figure 9). Figures 6 and 7 are the data obtained with the high stress rate equipment described earlier by Glaesemann<sup>2,12</sup>. As can be seen, while the log-log plot of these data seems to require three regions, a semi-log plot can be satisfactorily fit with two regions. The fit to an exponential law is in agreement with the results of Muraoke and Abe<sup>15</sup>. As indicated earlier however, they did not find region II behavior in tests on 50  $\mu\text{m}$  flaws. In Figure 8, data on fibers with two different strength levels (1 and 2 gram indents) have been shifted and are found to coincide. In Figure 9, all of the data on 1 gram indented fibers have been combined on a semi-log plot. In this plot, the open circles and open squares represent the data shown earlier in Figure 5.

## DISCUSSION

As can be seen from the above data, the use of a cube corner indenter gives strengths which correspond roughly to the proof test levels currently employed. The fit of the data to a single  $\sigma \sim P^{-1/3}$  line indicates that all of these indentation loads produce post-threshold flaws. Flaws resulting in inert strengths of approximately 700 MPa require a load of approximately 0.5 grams, while the development of room temperature strengths of this order requires loads of only approximately 0.06 grams. With these latter loads it is likely to be difficult to get good uniformity in the indentation process. In addition, modifications to the present tensile testing technique may be needed to maintain the mounting damage below that of the indentation damage. In this case, bending techniques as used by Lin and Matthewson<sup>14</sup> might be used. As pointed out earlier, the development of 'proof test' level flaws at such low indentation loads also emphasizes the need for extreme care in the handling of bare silica fibers.

In the regime of 'ordinary' times to failure, 1 to 100,000 seconds for fibers with strengths approximately 200 – 300 MPa, it was found that

two n-values (44 and 21) are required to fit the data within experimental error (a bend also was present in an exponential plot). At this strength level, the transition from one n-value to another occurs at  $t \sim 50$  seconds, but will be found to shift to shorter (longer) times for stronger (weaker) fibers. This may at least partly explain the variability found in the n-values for 'low strength' fibers<sup>16,17,18</sup>. Since the indents that produced the cracks studied here result from irreversible deformation, there are residual stresses associated with these cracks. Ordinarily this is expected to affect the magnitude of the n-value observed<sup>19,20</sup>. It is not clear whether such an effect is influencing the results observed here. While the exact representation of the moderate stress rate range are somewhat in doubt, the appearance of a second regime, a so-called 'region II – like' behavior, seems to be definitely confirmed.

Thus, in addition to the illustration of the advantages of such indentation techniques, this work reinforces the findings of Glaesemann, et al.<sup>1,2</sup>, that a second region appears in the strength-stress rate curves at a stress rate of  $\sim 1$  to 10 GPa/s for fibers having strengths of  $\sim 200$  to 700 MPa. While these data actually appear to indicate a third region at intermediate stress rates ( $\dot{\sigma} \sim 10^{-1}$  GPa/s), on an exponential plot this region is eliminated.

## CONCLUSIONS

We have shown that by using a cube corner indenter, strengths of the order of normal proof test levels can be obtained, with tight distributions (Weibull  $m \sim 30-70$ ). The fatigue behavior of such indented fibers ( $\sigma \sim 300$  MPa) indicates a transition in behavior at moderate stress rates (failure times  $\sim 50$  seconds) and may partially explain the apparent variability in the reported n-values for such low strength fibers.

High stress rate experiments show an apparent 'region II' behavior and a saturation of the strength at  $\sim 90\% \sigma_{IN2}$  for a stress rate of  $\sim 10^4$  GPa/s. This indicates that the 'two-region' model of Glaesemann, et al.<sup>1,2</sup> must be considered in evaluating proof test parameters. Additional studies are required in order to fully predict long time behavior.

## REFERENCES

1. T.A. Hanson and G.S. Glaesemann, J. Mat. Sci., **32**, 5305 – 5311 (1997).
2. P.T. Harvey, T.A. Hanson, M.G. Estep and G.S. Glaesemann, Proc. IWCS, 883- 888 (1997).
3. G.S. Glaesemann, Proc. IWCS, 698-704 (1992).
4. M.M. Bubnov, E. M. Dianov and S.L. Semjonov, Mat.Res. Soc. Symp. **244**, 97-101 (1992).
5. D.J. Wissuchek, MRS Proc. #531 (1998).
6. T. Breuls and T. Svensson SPIE, **2074**, 78 (1994).
7. C.R. Kurkjian, Mat.Res.Soc. Proc. **531** (1998).
8. Leco, Model M-400-G3, St. Josephs, MI 49085-2396.
9. Nano Instruments, Oak Ridge, TN 37830.
10. Instron, Canton, MA 02021.
11. J. T. Krause, and C. Shute, Adv. Ceram. Matls.,**3**, 118-121 (1988).
12. G. S. Glaesemann, Proc. SPIE, **2611**, 38-44 (1995).
13. C.R. Kurkjian S.L. Semjonov and O.S. Gebizlioglu, Proc. NFOEC, 73-80 (1997).
14. B. Lin and M. J. Matthewson, Phil. Mag., **74**, 1235-1244 (1996).
15. M. Muroake and H. Abe, Mechanics and Materials for Electronic Packaging, **1**, 141, ASME (1994).
16. C.R. Kurkjian, J.T. Krause and M.J. Matthewson, J. Lightwave Tech. **7**, 1360-1370 (1989).
17. M.M. Bubnov and S.L. Semjonov, Proc. MRS #531 (1998).
18. D. B. Marshall and B. R. Lawn, J. Am. Ceram. Soc., **63**, 532 (1980).
19. B.L. Symonds, R. F. Cook and B.R. Lawn, J. Matls., Sci, **18**, 1306 (1983).

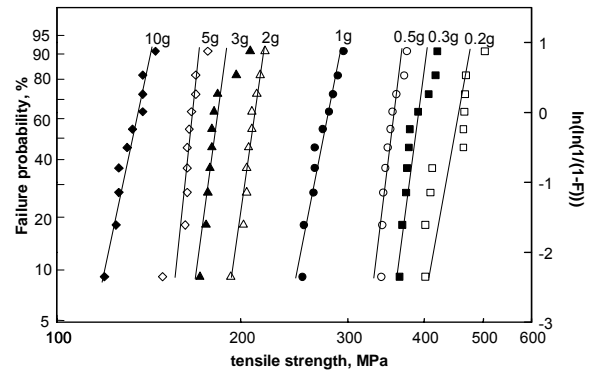


Figure 1. Strength of indented fibers at different indentation loads. Stress rate  $\sim 0.12$  GPa/s; relative humidity  $\sim 50\%$ .

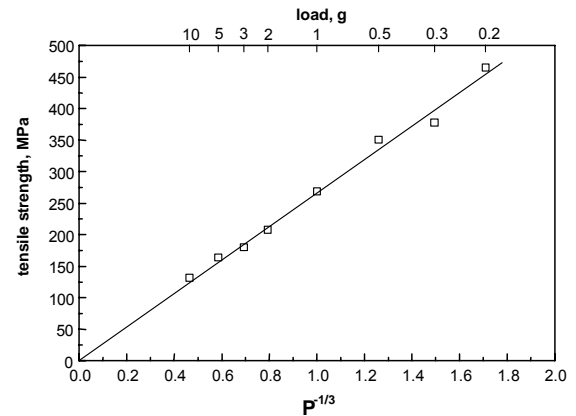


Figure 2. Dependence of median strength of indented fibers on indentation load.

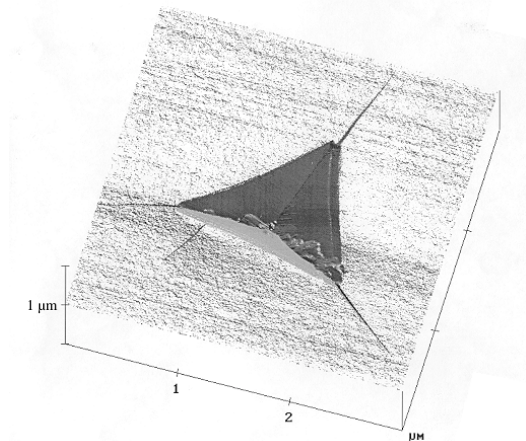


Figure 3. AFM image of 1 gram indent.

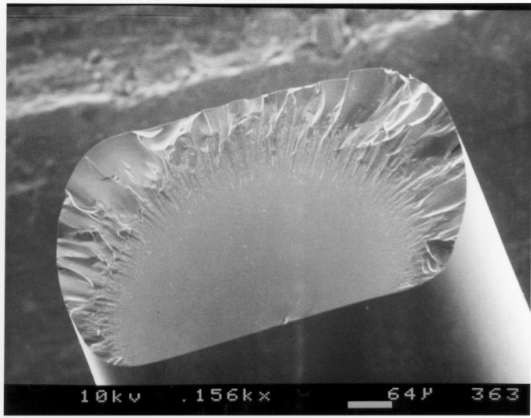


Figure 4. SEM image of fiber indented with 10 gram load.

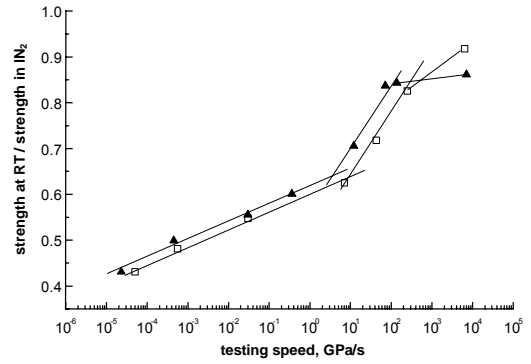


Figure 7. Median strength of indented fibers with high speed tester (semi-log plot). □ - 1 gram indent; ▲ - 2 gram indent.

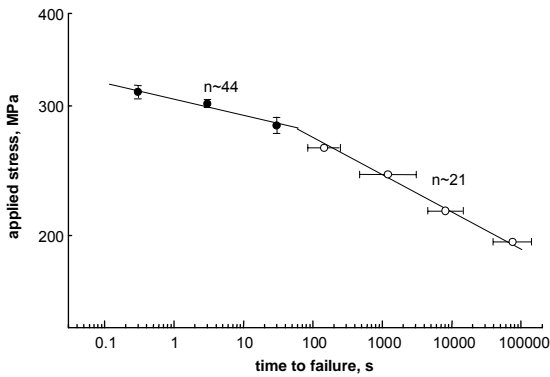


Figure 5. Combined plot of dynamic and static fatigue of 1 gram indented fiber at room temperature and ~ 50% RH (● - dynamic fatigue; ○ - static fatigue).

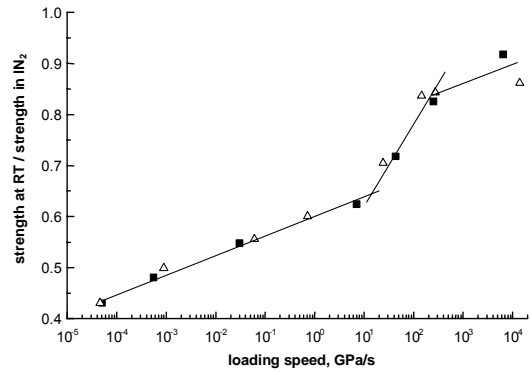


Figure 8. Median strength of indented fiber with high speed tester (semi-log plot). □ - 1 gram indent; ▲ - 2 gram indent (recalculated).

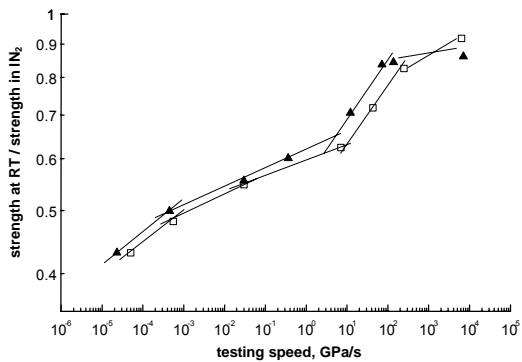


Figure 6. Median strength of indented fibers with high speed tester. (log-log plot). □ - 1 gram indent; ▲ - 2 gram indent.

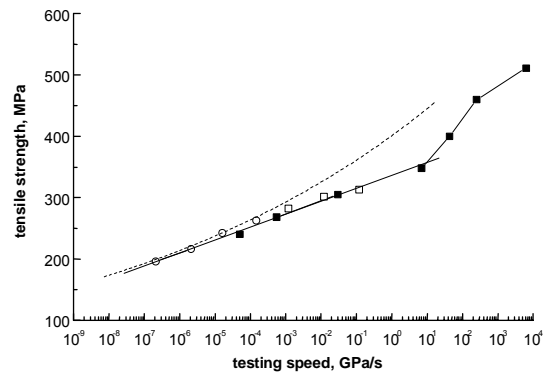


Figure 9. Combined plot of dynamic and static fatigue and high speed testing for 1 gram indented fiber. ■ - high speed; □ - dynamic fatigue; ○ - static fatigue; - - - n = 21.